Department of Precision and Microsystems Engineering

Design and Experimental Validation of Intracardiac Photoacoustic Catheter

Jimeet Dhaivat Oza

Report no : 2023.089
Coach : Dr.Ir. Sophinese Iskander-Rizk
Professor : Dr.Ir. Marcel Tichem
Specialisation : OPT
Type of report : Master's Thesis
Date : 27 October 2023

TU Delft Delft University of Technology

Challenge the future

Delft University of Technology

Jimeet Oza

Design and Experimental Validation of Intracardiac Photoacoustic Catheter

MASTER'S THESIS

submitted to
Delft University of Technology

Supervisor Comitteee
Dr.Ir. Sophinese Iskander-Rizk - Daily Supervisor
Dr.Ir. Marcel Tichem - Supervisor and Chair

Delft

Abstract

Atrial fibrillation is a cardiac arrhythmia resulting from abnormal electrical conduction and impulse formation within the atria. To address this condition, a minimally invasive procedure called cardiac ablation is performed. Real-time visual feedback during this procedure plays a critical role in determining its success.

Photoacoustic imaging is a technique capable of providing real-time visual feedback. Integrating photoacoustic capabilities into existing Radiofrequency ablation catheters poses a significant challenge, which this thesis addresses. The proposed integrated solution employs optical fibers for light delivery and an ultrasound transducer for signal reception.

This work investigates the design of two light delivery systems for integrated photoacoustic-guided surgery. Monte Carlo simulations are employed to study three-dimensional light propagation in tissue, informing the catheter design specifications. Optimal fiber distances and orientations within the catheter are determined based on normalized fluence values and illumination spot size—critical parameters for assessing the amount of delivered light, its area of coverage, and depth of penetration. The methodology presented applies to various photoacoustic applications.

The simulation study was able to successfully inform design specifications and it was able to establish a relation between design variables and the evaluation criteria such that it can be referred to for future designs. The comparative study yielded a better-performing design configuration and its optimal specifications were found out. This proves the use of a simulation-based evaluation to design a photoacoustic intracardiac catheter. In the final phase of this research, an experiment is set up to validate the light delivery of the design, which provides a clear outlook for the future of these designs into fabricated products.

Acknowledgements

With the completion of this thesis, I mark the end of my journey as a master's student pursuing an MSc in Mechanical Engineering (High-Tech Engineering) at TU Delft. Over the course of a year dedicated to this project, I am thankful for the support and guidance provided by the following individuals:

First and foremost, I would like to express my gratitude to my daily supervisor, Sophinese. She has been my constant support throughout my thesis. She introduced me to this topic and allowed me the freedom to choose my approach. Her deep understanding and knowledge of the subject were invaluable in providing me with clear insights. Our discussions, where we explored various ideas and tackled the challenging aspects of my research, were always enjoyable. Her meticulous attention to detail consistently pointed me in the right direction, helping me navigate the complexities of my work.

I also want to acknowledge my supervisor and chair, Marcel, who encouraged and guided me on the path of research, even when I faced challenges in terms of management and planning. His guidance on simplifying complex topics and presenting my work with scientific rigor was crucial in maintaining the quality and depth of my research. Despite their busy schedules, both supervisors have kept their patience with me and addressed my doubts.

I extend my appreciation to the Ph.D. researchers in the OPT research section for their knowledge-sharing and to the lab support staff for their assistance in fulfilling my requirements and providing necessary lab components that would have otherwise been challenging.

Last but not least, my heartfelt thanks go to my family and close friends, both in India and here in the Netherlands, who have always supported me, fulfilled my small requests, and brought moments of joy when I needed them.

Jimeet Dhaivat Oza

Delft, 13 October 2023

Contents

1 Introduction **4**
- 1.1 Background . . . 4
- 1.2 Problem Definition . . . 11
- 1.3 Research Objectives . . . 11
- 1.4 Thesis Outline . . . 12

2 Literature Study **13**
- 2.1 Photoacoustics . . . 13
- 2.2 State-of-the-art photoacoustic catheters . . . 14
- 2.3 Key findings in literature . . . 18

3 Design **19**
- 3.1 Design configuration . . . 19
- 3.2 Design Methodology . . . 20
- 3.3 Monte Carlo simulations . . . 21
- 3.4 Results and discussion . . . 24
- 3.5 Final Design . . . 29

4 Experiment Methods **32**
- 4.1 Experimental setup . . . 32

5 Conclusions and Recommendations **36**
- 5.1 Conclusions . . . 36
- 5.2 Recommendations . . . 37

1 | Introduction

A good way to judge the significance level of any topic is by checking if it is commemorated with a special day. In this light, the heart, being crucial to our well-being, is celebrated on the 29th of September, known as World Heart Day. This observance serves as a platform to elevate awareness about Cardiovascular Diseases (CVD), emphasizing their prevention and management. According to the World Health Organization, 32 percent of total deaths per year are caused due to Cardiovascular diseases, and these only increase over age.

The onus for treatment then falls upon the hands of technology. Not just any technology but something that is safe, relatively quick, and affordable and doesn't scare away the patients. The development of minimally invasive treatment procedures has mitigated many of these medical challenges. Constant improvements in technology and imaging guidance have made treating difficult conditions and areas of the body with less pain, damage, and time. In minimally invasive interventions, catheters—slender, pliable tubes—are introduced through a minor incision to administer localized treatment to the target organ.

Catheter-based treatments have a great advantage over cardiac surgery. They can be done frequently and do not require an observation time of a few days, In fact, in most cases patients are also not required to stay overnight. On the other hand, open heart surgeries require hospitalization for at least a week and full recovery might take up to a year. Not to mention, the physical trauma of these surgeries is immense. Minimally invasive procedures offer the advantage of removing the sense of discomfort induced by open-heart surgeries while also being the more cost-effective alternative.

1.1 Background

Atrial Fibrillation (AF) is a condition that can be experienced by people of any age group. This condition takes away control of the heart rhythm. The upper chambers of the heart are responsible for generating electric impulses to regulate the heartbeat. Atrial Fibrillation occurs when other areas of the heart start sending electrical impulses as shown in Figure 1.1. When this happens, the blood is not pumped out effectively, which leads to the formation of blood clots. If a clot travels through the body or, more dangerously, to the brain, the consequences can be fatal. Inefficient pumping can also lead to heart failure, although this is relatively less common. In this case, the heart beats inefficiently, causing blood to back up in the heart and resulting in fluid in the lungs.

AF can be treated in many ways, and the most appropriate treatment depends on the type, frequency, and severity of the AF, as well as the patient's overall health. Some common

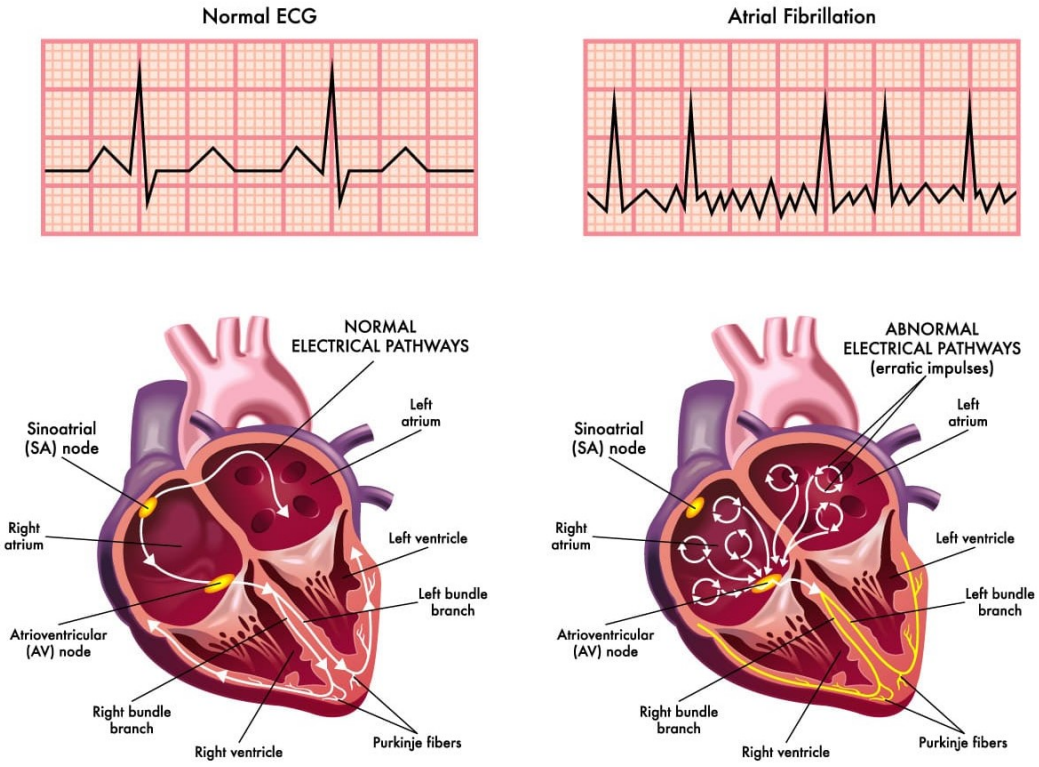

Figure 1.1: What happens during AF inside the Heart [1]

treatment methods include:-

- Medications: Doctors may prescribe medications to control heart rate, reduce the risk of blood clots, or restore normal heart rhythm.
- Cardio-version: This is a procedure in which an electrical shock is delivered to the heart to restore normal heart rhythm.
- Catheter Ablation: Ablation is a procedure in which a catheter is used to deliver radiofrequency energy or cryotherapy (cold energy) to destroy small areas of heart tissue that are causing abnormal electrical signals.
- Surgery: In some cases, open-heart surgery may be necessary to treat AF.

Catheter Ablation is a medical procedure used to treat atrial fibrillation. The process involves the use of a catheter, which is inserted through a small incision in the groin or arm and guided through the blood vessels to the heart.

Once the catheter reaches the heart, a specialized tool on the tip of the catheter is used to deliver energy, such as heat or cold, to the specific area of the heart responsible for causing the arrhythmia. This energy damages a small area of heart tissue (termed a Lesion) that is causing the abnormal heart rhythm and restores normal heart function. The process can be visualized in Figure 1.2

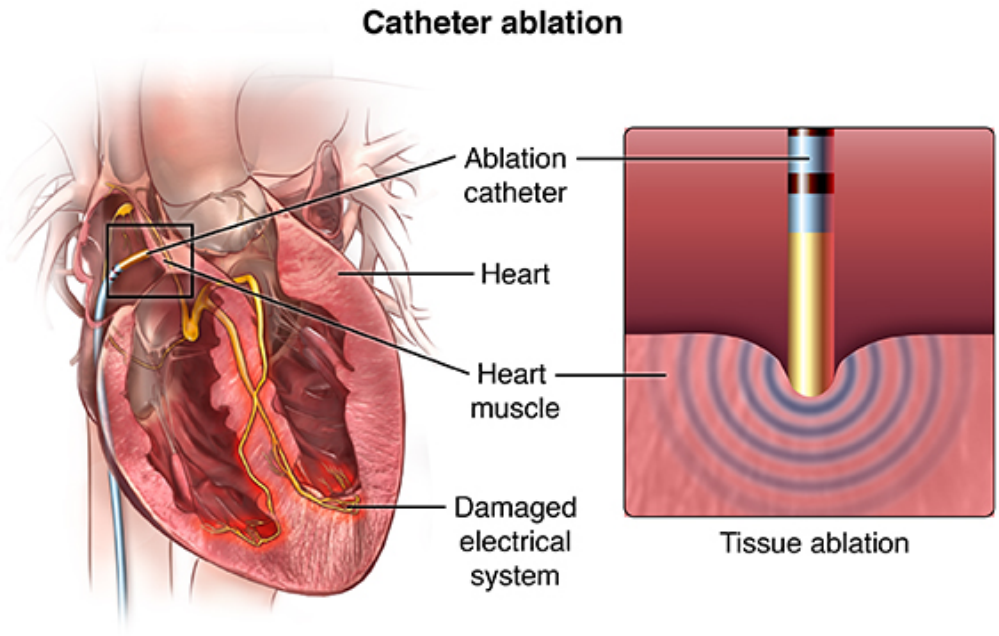

Figure 1.2: Catheter Ablation procedure in action where the small catheter tip is seen using energy to burn tissue/form lesions [2].

The ablation process can be broken down into different operations with each operation having a specific purpose and requiring different methods to achieve the purpose. The first step involves inserting a catheter into a peripheral vein and guiding it to the heart using fluoroscopy. In the second step, a combination of imaging techniques including fluoroscopy, intracardiac echocardiography, and electroanatomical mapping is used to navigate the catheter to specific regions of the heart and confirm that the catheter is in contact with the tissue. Finally, ablation is performed using the energy source. The process of creating a lesion is also monitored via different imaging techniques and feedback is obtained via measuring the contact force of the catheter to the tissue.

Feedback during catheter ablation

Feedback was introduced in the catheter ablation process, including RF catheter ablation, to improve the safety and efficacy of the procedure. Prior to the use of feedback mechanisms, the operator would have to rely on subjective factors such as the catheter's appearance, the sensation of resistance when moving the catheter, or the patient's response to the procedure to determine the location and extent of the ablation lesion [3]. This approach was less precise and could result in incomplete or excessive ablation, which can lead to complications such as bleeding, perforation, or damage to adjacent structures.

Initially, Impedance measurement was introduced as a means of obtaining feedback. It is a technique used to measure the resistance to the flow of RF energy through the heart tissue. As the RF energy is delivered, the tissue temperature increases and the resistance to the energy flow decreases. By measuring the change in resistance, the catheter system can estimate the temperature of the tissue and monitor the progress of the ablation procedure. Another

prominent method that was used is Contact force sensing. It became a very effective method as it was statistically proven to be effective in reducing AF recurrence during the first year after PVI [4], [5]. Figure 1.3 refers to an integrated Contact force sensing Ablation catheter which uses a precision spring.

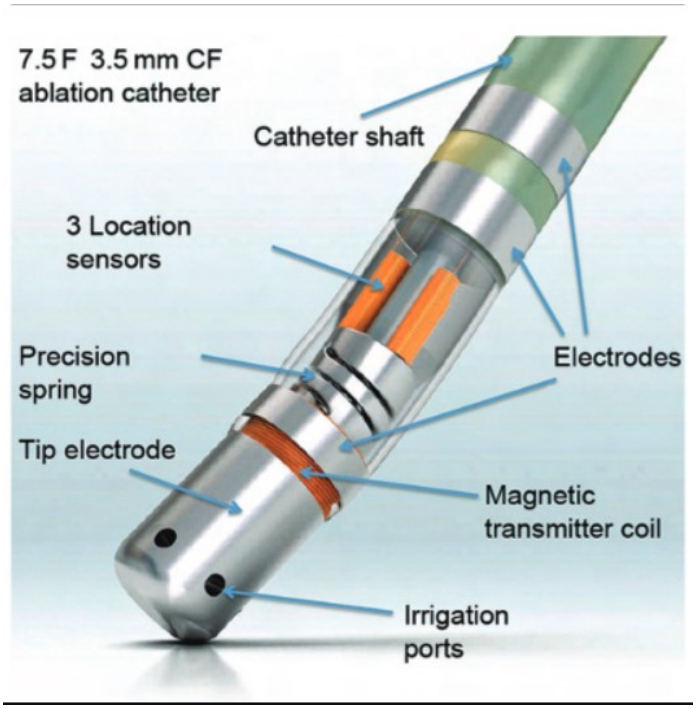

Figure 1.3: An example of Contact force sensing Catheter with an irrigation tip [6]

A summary of feedback mechanisms used in radiofrequency (RF) catheter ablation procedures, including:

1. Impedance monitoring: This technique measures the resistance to the flow of RF energy through the heart tissue. By measuring the change in resistance, the catheter system can estimate the temperature of the tissue and monitor the progress of the ablation procedure.
2. Contact force sensing: This technology uses sensors located at the catheter tip to measure the amount of force applied to the tissue. The data obtained by the sensors is displayed on the operator's console in real-time, allowing the operator to adjust the contact force as needed to optimize the ablation.
3. Electrogram analysis: This feedback mechanism uses sensors located on the catheter to measure the electrical activity of the heart tissue during the ablation procedure. The data obtained can help the operator to locate the source of the arrhythmia and determine the success of the ablation.
4. Temperature monitoring: This technique uses sensors on the catheter to measure the temperature of the heart tissue during the ablation procedure. The data obtained can help the operator to adjust the energy delivery parameters to optimize the ablation and avoid complications.

Imaging and guidance in Catheter Ablation

In the process of catheter ablation, imaging and guidance hold a pivotal role in visualizing the intricate anatomy of the heart and guiding catheters to precise target locations. This critical function substantially reduces the risk of complications and elevates the overall success rate of the procedure. Imaging serves as an indispensable feedback tool, enhancing the precision of ablation procedures. Several imaging techniques, including fluoroscopy, intracardiac echocardiography, and 3D mapping, have been utilized for guidance, each offering unique advantages and encountering specific limitations.

In current practice, Cardiologists rely on multiple sensor data to gauge the endpoint of ablation and mitigate potential risks to patient safety. However, due to the dynamic nature of the procedure and the presence of factors such as fat and vessels, the energy delivery profile may need to be altered. This complicates the interpretation of various sensor readouts and can result in incomplete lesion profiles.

Current techniques used in imaging

1. **Biophysical models and Impedance measurements** - Biophysical models are mathematical models used to predict the effect of ablation on the heart tissue based on physical and physiological parameters, such as tissue conductivity and blood flow. Impedance measurements, on the other hand, involve monitoring changes in the electrical impedance of the tissue during ablation to provide an indication of lesion formation.

   They are limited in their ability to provide direct visualization of the lesion as it is being formed. They provide an indirect measurement of the lesion's characteristics based on the changes in the electrical properties of the tissue during ablation. This can lead to inaccuracies in lesion size and location, as well as difficulty in distinguishing between healthy and ablated tissue. Additionally, these methods require specialized equipment and expertise, which can limit their widespread adoption in clinical practice.

2. **Fluoroscopy** - Fluoroscopy is a medical imaging technique that uses X-rays to obtain real-time moving images of the internal structures of a patient's body. During a fluoroscopy procedure, a continuous X-ray beam is passed through the body part being examined and the images are captured on a screen.

   It lacks depth information and has risks associated with ionizing radiations.

3. **X-Ray** - X-ray is used to visualize the anatomy of the heart and the blood vessels in real-time. This provides the interventional cardiologist or electrophysiologist with a clear view of the patient's cardiac structures, including the chambers, valves, and blood vessels, which helps them navigate the catheter to the target area.

4. **Electroanatomical mapping** - Electroanatomical mapping (EAM) is a technique to create a three-dimensional map of the heart's electrical activity. It uses a catheter with multiple electrodes to measure electrical signals from inside the heart and creates a detailed map of the heart's electrical activity.

5. **Intracardiac Echocardiography** - Intracardiac Echocardiography or Intracardiac ultrasound (ICE) is a medical imaging technique that uses a catheter-based probe to produce detailed images of the heart's internal structures. The catheter is inserted into a

blood vessel and guided to the heart, where it emits high-frequency sound waves that bounce off the heart's tissues and are then picked up by the probe.

It requires skilled operators thus increasing the dependence on operators. It acquires images only from a local reference frame which may not provide a complete understanding of the overall cardiac anatomy and the location of the catheter tip in relation to it.

6. **Optical Coherence Tomography** - Optical Coherence Tomography (OCT) is a high-resolution imaging technique that uses light waves to create detailed cross-sectional images of tissues. OCT relies on a near-infrared laser as its light source, chosen for its ability to penetrate tissues safely. The laser light is split into two beams: the sample beam and the reference beam. The sample beam is directed towards the tissue under examination, while the reference beam is aimed at a reference mirror.

   Interference plays a central role in OCT. As the sample beam reflects back from different depths within the tissue and the reference beam reflects from the reference mirror, these two beams are recombined. The interference between the two beams generates an interference pattern, with the reflected light waves either reinforcing or canceling each other out. This pattern holds vital depth information based on the time it takes for light to travel to the tissue and back.

   Optical Coherence Tomography (OCT) has limitations in catheter ablation procedures for conditions like atrial fibrillation. First, it offers limited depth penetration, hindering the visualization of deeper lesions. Third, real-time imaging challenges can arise due to delays in image acquisition and processing.

Monitoring lesions during catheter ablation procedures remains a critical but challenging task, as no single method has been found to meet all necessary criteria. Lesion monitoring is crucial because its success or failure can determine the outcome of the procedure. Unfortunately, there are still cases where under-ablation leads to AF recurrence, while over-ablation can cause heart damage as seen in Figure 1.4 even after technological developments. Contact force and impedance measurements are useful, but they only provide indirect measurements that require skilled operators to interpret and visualize accurately. As ablation technologies continue to advance and improve energy delivery, it is essential to ensure that feedback methods keep pace with these changes. By doing so, ablation procedures can be optimized, the risk of complications can be reduced, and patient outcomes can be improved.

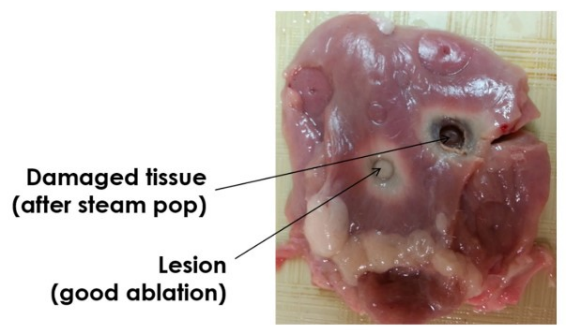

Figure 1.4: An example of damage caused due to Radiofrequency [7]

Photoacoustic imaging serves as a pivotal technique for real-time lesion monitoring during catheter ablation procedures. This innovative approach involves the targeted delivery of laser light to the tissue, where it is absorbed. This absorption event triggers rapid thermal expansion within the tissue, resulting in the generation of acoustic waves. These acoustic waves are captured and recorded by an ultrasound transducer, forming the basis of the photoacoustic imaging process. This would, in theory, allow clinicians to visualize and monitor the formation, progression, and characteristics of lesions within the tissue offering invaluable insights for catheter ablation procedures.

Lesion Visualization with Photoacoustic

The visualization of lesions in cardiac ablation fundamentally encompasses three key aspects:

- Lesion Progression: Lesion progression refers to the dynamic development and evolution of a lesion over time. Monitoring how a lesion changes can provide valuable insights into its behavior and the effectiveness of the procedure.
- Lesion Depth: Lesion depth denotes the extent to which tissue has been affected or burned during the ablation process. Understanding lesion depth is crucial for determining whether a lesion has been adequately treated or if adjustments are needed. An accurate assessment of lesion depth ensures that the procedure neither under-ablates nor over-ablates the tissue, striking a critical balance for optimal outcomes.
- Lesion Continuity: Lesion continuity refers to the uninterrupted or connected nature of a lesion within a tissue or organ. Maintaining lesion continuity, particularly in procedures like pulmonary vein isolation (PVI), is important for effectively isolating the targeted area.

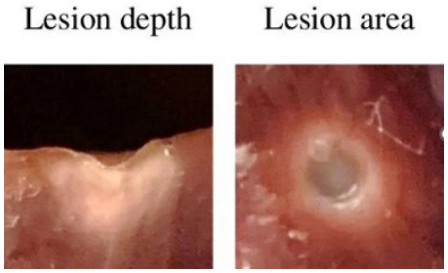

Figure 1.5: Lesion created on a tissue [8]

Fluence and illumination area are important criteria in visualizing lesions during a cardiac ablation procedure. Fluence refers to the amount of energy or light delivered per unit area. It is typically measured in units of energy per square centimeter (e.g., joules per square centimeter or W/cm^2). The illumination area or illumination spot is the area that is exposed to light or the area in which the light is delivered.

The importance of fluence and illumination area in visualizing lesions cannot be overstated. These factors are pivotal in assessing lesions post-creation, aiding in the accurate evaluation of lesion size, shape, and depth. Adequate fluence and illumination area enhance lesion identification against healthy tissue, particularly when dealing with subtle or small lesions. Moreover, they play a crucial role in preventing over-treatment, thereby safeguarding patients

from unnecessary harm. By optimizing imaging technology settings based on specific lesion characteristics and patient anatomy, healthcare providers can ensure the highest quality of lesion visualization, ultimately leading to more successful treatments of heart rhythm disorders while reducing complications.

1.2 Problem Definition

Feedback information during catheter ablation forms the basis of the success rate of the procedure. It has a large influence over successful surgery. Since the current methods are an indirect way of gaining feedback, research for direct visual feedback has been taking momentum. Several attempts that have been made in this field do not fully solve the problem. OCT imaging provides a good blend of compactness and integrability into the ablation catheter but fails to get the required depth information. Photoacoustics has proved to be the solution for lesion monitoring in terms of depth information and functional information but no catheter design in literature has achieved the required field of view (illumination area), fluence, Signal to noise ratio, Contrast to noise Ratio, and temperature profile without compromising the clinical standards for the size of the catheter. In order to include all functionalities it is important to manage the design space that is available inside the catheter. Photoacoustic light delivery is an important aspect to consider for designing integrated catheters. An optimal position and location of light source is necessary in order to visualize the lesions properly and hence there needs to be a flexible design method that can be used to design the light delivery system such that it can give further information on how much space is left for other functionalities.

1.3 Research Objectives

The research aims to design and experimentally validate the light delivery system for an integrated photoacoustic ablation catheter, addressing specific functional requirements:

- Monitoring of lesions, including lesion depth, lesion continuity, and lesion temperature profile.
- Adherence to clinical standards, encompassing the necessary compliance and catheter diameter (3-4mm).
- Integration of sensing functionalities, allowing for the incorporation of an ultrasound sensor to gather relevant information.
- Preservation of advanced features, such as catheter cooling, without compromise.

The criteria on which the design specifications will be based are taken from literature and they will be used to inform a decision on the location and orientation of optical fibers that are used to deliver the light in photoacoustic catheters. These criteria are:-

1. The Catheter must create an illumination spot size of more than 4.5mm so that it is able to monitor the whole area of the lesion and also to visualize whether lesion continuity is achieved.
2. It must maintain fluence levels to generate a detectable photoacoustic signal. There is no threshold for this value but previous studies [9] have shown the $6mW/cm^2$ was able

to generate the PA signals and so was $120 mW/cm^2$. It depends on at which depth it is measured but for this study, the measurements will be at a depth that is 80% of the depth of the lesion so it is confirmed that enough intensity of light is reaching to create a lesion depth profile.

3. It must be suitable for multiple wavelengths as it is proven to have achieved a diagnostic accuracy of 97 percent and displays a sensitivity of 88 percent and specificity of 100 at detecting lesions [9].

1.4 Thesis Outline

The current chapter offers an overview of the catheter ablation procedure, including its techniques, limitations, and existing gaps. With the central focus of this thesis being on photoacoustic (PA) technology, the chapter 2 delves into a review of state-of-the-art PA catheters in research. This chapter explores their design characteristics, advantages, and limitations, contributing to a detailed understanding of the design requirements.

chapter 3 elaborates on the the different design concepts and establishes a design methodology. The final design is then selected among the two design concepts(configurations) and its optimal position of light source is determined.

chapter 4 centers on the experimental phase aimed at developing tools and methods to facilitate the experimental validation of the proposed design. This marks the end of the research and the chapter 4 is followed by the conclusions and reccomendations.

2 | Literature Study

2.1 Photoacoustics

Photoacoustic is a phenomenon where light is absorbed by a material (in this case a tissue), leading to the generation of acoustic waves that can be detected and used to create images or perform other measurements. Photoacoustic involves the use of laser light to penetrate into a sample, such as biological tissue, and be absorbed by specific molecules, such as hemoglobin or melanin, which contain chromophores. Chromophores are a chemical group or a molecule that absorbs light. They can be targeted to visualize specific structures or molecules in biological tissue. For example, hemoglobin, which is a chromophore that absorbs light in the near-infrared range, can be used to visualize blood vessels and detect oxygen saturation levels in tissue. This absorption leads to a local temperature increase, which in turn causes the material to expand and generate acoustic waves. These acoustic waves can be detected by sensitive microphones or other sensors and used to create images of the tissue as seen in the Figure 2.1.

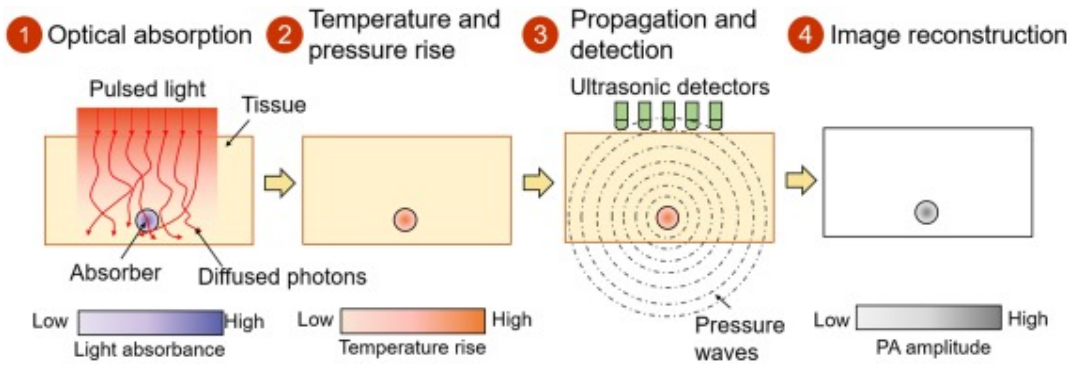

Figure 2.1: Concept of Photoacoustics imaging [10]

The pertinent question arises: Why should photoacoustic imaging be adopted in the medical field, given the already widespread use of other imaging and mapping techniques such as fluoroscopy, ultrasound, and MRI?

Photoacoustic imaging is used for several reasons, including its ability to provide high-resolution images of biological tissue with good contrast. Here are some of the key advantages of photoacoustic imaging:

1. High resolution: Photoacoustic imaging can provide high-resolution images of biological

tissue structures, such as blood vessels and tumors, with better contrast than other imaging modalities like ultrasound.

2. Specificity: Photoacoustic imaging can be used to detect and monitor the concentration of specific molecules, such as glucose or oxygen, in real-time. This specificity can be useful in diagnosing and monitoring diseases like cancer and diabetes.
3. Non-invasive: Photoacoustic imaging is a non-invasive imaging modality that does not use ionizing radiation, making it safer for patients than other imaging techniques like X-rays.
4. Deep penetration: The photoacoustic effect allows for light to penetrate deeper into biological tissue, up to several centimeters, enabling visualization of structures that would be difficult to see using other imaging modalities.
5. Versatility: Photoacoustic imaging can be used for a variety of applications, from basic research to clinical diagnosis and treatment monitoring, as well as in fields like materials science and environmental monitoring.

Overall, the benefits of photoacoustic imaging make it a promising modality for a range of medical and scientific applications.

2.2 State-of-the-art photoacoustic catheters

Photoacoustic imaging has shown great potential and rich history in several applications. Earlier it was only used as a tool for small animal imaging, molecular imaging, and vascular network imaging. Next, it was thought to make a significant addition to procedures and surgeries provided the technology itself also advanced in order to support the shift to photoacoustics. Today, a lot of technologies have caught up and now photoacoustics is being used in a variety of applications. It provides a lot of benefits for surgical guidance because its penetration depth exceeds purely optical imaging methods. Furthermore, its spatial resolution is similar to ultrasound imaging, and it has the ability to determine functional information based on changes in optical properties.

Lesions involve more than just the surface layers; this is where photoacoustics shows promise. Photoacoustics provides functional and visual feedback by creating images based on light and sound waves generated by tissue. This technology has the potential to meet all the necessary criteria for lesion monitoring and feedback, making it an exciting development in the field of catheter ablation for Atrial Fibrillation.

PA contrast for lesion imaging

Introducing a completely new system is not easy and it integrated itself step by step. The first few studies were focused on PA contrast for lesion monitoring. Bouchard et al [11] used photoacoustic imaging to characterize the optical properties of Radiofrequency ablation (RFA) lesions in cardiac tissue. The researchers found that photoacoustic imaging could accurately differentiate between viable and necrotic tissue based on their optical absorption spectra, providing a potential means of monitoring the efficacy of RFA procedures. These results were echoed by Dana et al [12] who also found that photoacoustic imaging could accurately identify the size and location of the lesions, as well as distinguish between viable

and necrotic tissue. Visualization of lesions was also boosted when Pang et al [13] developed a three-dimensional (3D) optoacoustic (OA) monitoring system for real-time visualization of lesion formation during RFCA procedures. They demonstrated the feasibility of the system in a tissue-mimicking phantom and ex vivo porcine heart experiments. They found that the OA signal amplitudes increased with increasing laser fluence and that the OA images were able to visualize the ablation lesions in 3D.

Although the previous results were promising they were done in ventricular tissue which cannot be directly adapted for atrial fibrillation. Iskander-Rizk et al [9] characterized the photoacoustic signal from fresh and ablated porcine left atria tissue specimens over the range of 410 to 1000 nm. It was concluded that dual-wavelength ratio-based imaging removes the need to model the PA signal variation with tissue attenuation and temperature, which are relatively independent of temperature.

Recently, Gao et al [14] found that the PA signal amplitudes increased with increasing laser fluence and that the PA images were able to visualize the ablation lesions. This study was succeeded by a cardiac-gated spectroscopy PA imaging study [15] where they focused on the development and in vivo demonstration of a spectroscopic photoacoustic imaging technique for visualizing ablation-induced necrotic lesions in a beating heart. The spectroscopic approach used in the study enabled differentiation between the necrotic lesion and surrounding healthy tissue based on their unique absorption spectra. Some results from these previous literature are detailed in Figure 2.2.

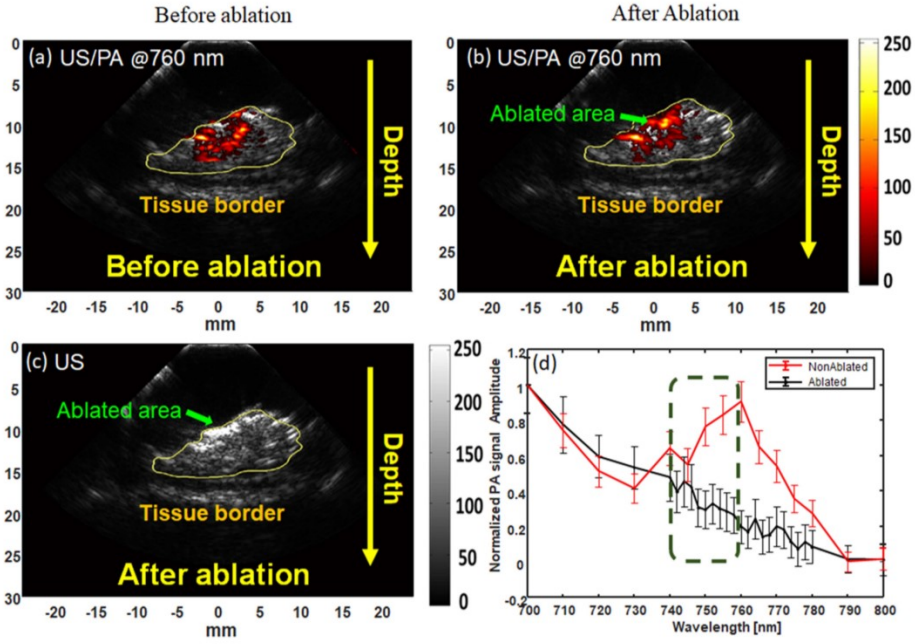

Figure 2.2: Tissue distinguishing capability of US versus that of US/PA. and a graph showing the Variation of the mean of PA signal amplitude in the spectrum (λ = 740–760 nm) acquired from the surface of the tissue. Results indicate a distinguishable trend between ablated and non-ablated tissue regions [16]

PA Integrated Ablation and Imaging Catheter

After successfully cementing lesion imaging through PA, the next step involved integrating the technology with the ablation catheter so that real-time imaging is possible. Iskander-Rizk et al [17] described two designs (Figure 2.3) of PA-integrated ablation and imaging catheters and their performance in terms of light delivery, fluence, etc. A continued study [18] was able to demonstrate the earlier findings in real-time with a simple and easy-to-integrate device. The initial designs proposed by [17] had the optimum clinical size but they had a lesser area probed in comparison to Rebling et al [19] who developed an integrated catheter for simultaneous RF and PA monitoring that also focused on increased illumination area and fluence. They demonstrated the feasibility of the system in a tissue-mimicking phantom and ex vivo porcine heart experiments. They found that the PA signal amplitudes increased with increasing laser fluence and that the PA images were able to visualize the ablation lesions in real-time. They also found that the catheter was able to perform RF and PA monitoring simultaneously without affecting the ablation efficacy but there was always a tradeoff between the diameter of the catheter and the illumination area. The downside to this catheter was that its diameter was $6mm$ which is more than the clinical standards. Gao et al [14] were able to confine the Ultrasound (US) probe, optical fiber, and RF electrode all in one catheter as shown in figure Figure 2.4. But, they couldn't provide the required depth information as the single US probe was not efficient in collecting all the PA signals. Furthermore, it was found with this arrangement, that the heat transfer from PA and RF contact would excessively ablate the tissue. To overcome this challenge, the next set of designs focused on integrating laser ablation and PA imaging.

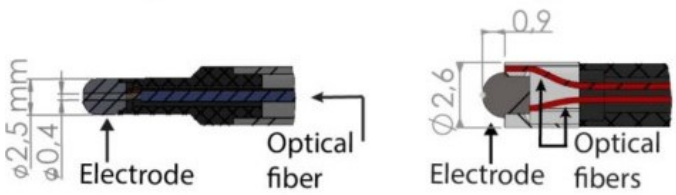

Figure 2.3: Early PA integrated RF Catheters [17]

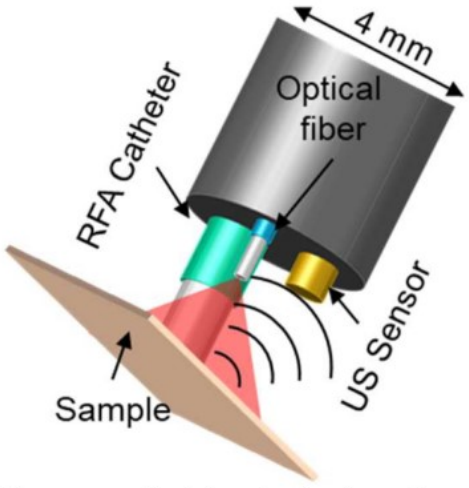

Figure 2.4: An integrated catheter with Ultrasound probe [14]

A lot of integrated catheters were developed by Basij et al. [20] [16] in which their catheter featured a diameter of $6mm$ and utilized 7 optical fibers to combine laser ablation and photoacoustic imaging with a single US probe. The side-facing design includes 6 pulsed laser fibers for photoacoustic imaging and one continuous wave laser fiber for ablation. By using this design, they were able to achieve more uniform light delivery and higher laser fluence.

However, there were some limitations to this design. Specifically, the catheter exceeded the $4mm$ diameter clinical standard and had some limitations in terms of tissue ablation efficiency due to the side-facing design. Nonetheless, this work represents an important step forward in the development of integrated catheters for use in catheter ablation procedures. A PA laser ablation catheter design concept is shown in Figure 2.5

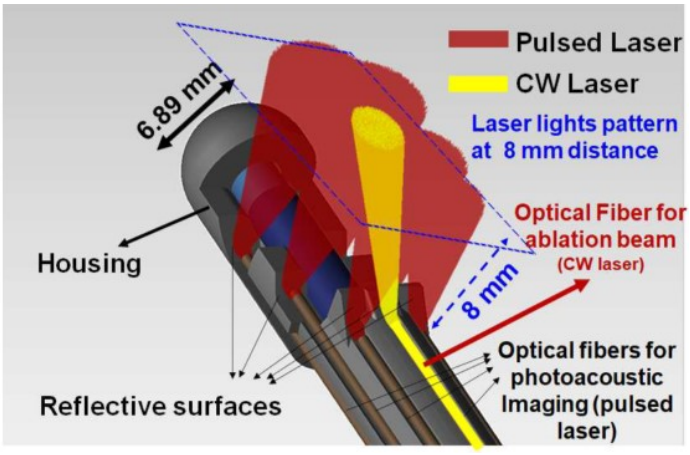

Figure 2.5: Integrated PA and Ablation Catheter [16]

2.3 Key findings in literature

After going through all the catheter designs and its limitations, it is clear that the most challenging aspect of design is to stay within the clinical standards. There are different ways in which the components inside the catheter can be arranged and multiple concepts are possible. Hence, It is important to develop design methodology such that it is able to take into consideration multiple design possibilities and provides a great way to judge the results before going into experimental phase. Keeping this mind, a simulation based design methodology is being employed in this research in the next chapter.

3 | Design

Within a multifunctional catheter assembly, the optimization of available design space is critical for the integration of various components such as ablation electrodes, optical fibers, ultrasound transducers, force sensors, and irrigation channels, all within predetermined design constraints. This project concentrates on optimizing the light delivery subsystem, essential for initiating photoacoustic phenomena. The subsystem's effectiveness is contingent on the accurate positioning and alignment of optical fibers relative to target tissue. Therefore, an exhaustive analysis of the light delivery subsystem is necessary to evaluate the available space for additional essential components. This chapter primarily focuses on achieving efficient light delivery while meeting design constraints, emphasizing on fluence and illumination area. Subsequent analyses will investigate two discrete design configurations via simulation.

3.1 Design configuration

The selection of design configurations for the catheter is based on the positioning of the electrode, a determining factor for subsequent design decisions. From the existing literature, it is evident that an integrated photoacoustic (PA) catheter necessitates three essential components: a radiofrequency (RF) electrode, an optical fiber for the light source, and an ultrasound sensor. Given that the electrode occupies significant space within the catheter, the design is primarily influenced by its placement. Conventionally, the electrode is positioned centrally in the catheter, but alternative designs have also explored electrode placement at an offset or side of the catheter seen in Figure 2.4. Consequently, various configurations are possible. To streamline the simulation study, this research focuses on two cases, one with the electrode at the center and the other with an offset configuration, thereby encompassing both variations.

Both configurations employ a standard 7F (2.3 mm) electrode diameter, with the assembly's total diameter set at 3.5 mm. Variables under consideration include electrode separation distance (d_t), fiber-electrode tip distance (d_h), and fiber orientation and launching angle. By manipulating these variables, simulations aim to identify configurations of these variables that yield optimal fluence over the lesion area and are able to illuminate the required spot size.

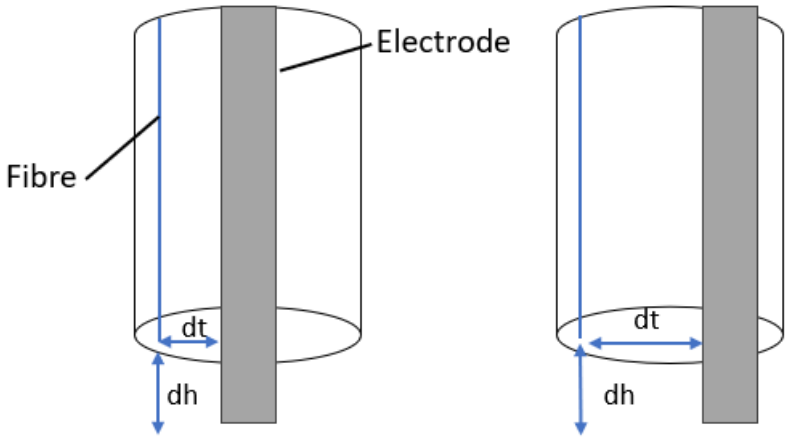

Figure 3.1: Two Design configuration

3.2 Design Methodology

Figure 3.2 illustrates the design methodology employed. An initial set of design constraints were established post-literature review to facilitate the development of an integrated catheter. These were primarily on the geometric constraint for the catheter. Evaluation criteria were subsequently determined based on the fluence and illumination area, followed by the definition of initial design configurations and variables serving as inputs for Monte Carlo simulations. These simulations inform the final Computer-Aided Design (CAD) model, which also includes placeholders for other modalities such as ultrasound sensors and force sensors.

When simulating how light interacts with biological tissue, the initial stage usually involves determining how light is distributed within the tissue based on its optical characteristics when illuminated. This distribution of light is determined by solving the radiative transfer equation (RTE). Monte Carlo methods are employed to solve this equation. In this approach, light is represented as photon packets that gradually get absorbed as they traverse the medium. Along the way, they also experience random scattering, the likelihood of which depends on the local optical properties of the medium.

The MCmatlab package developed by Anderson et al. [21] is utilized to do the Monte Carlo Simulations for this project.

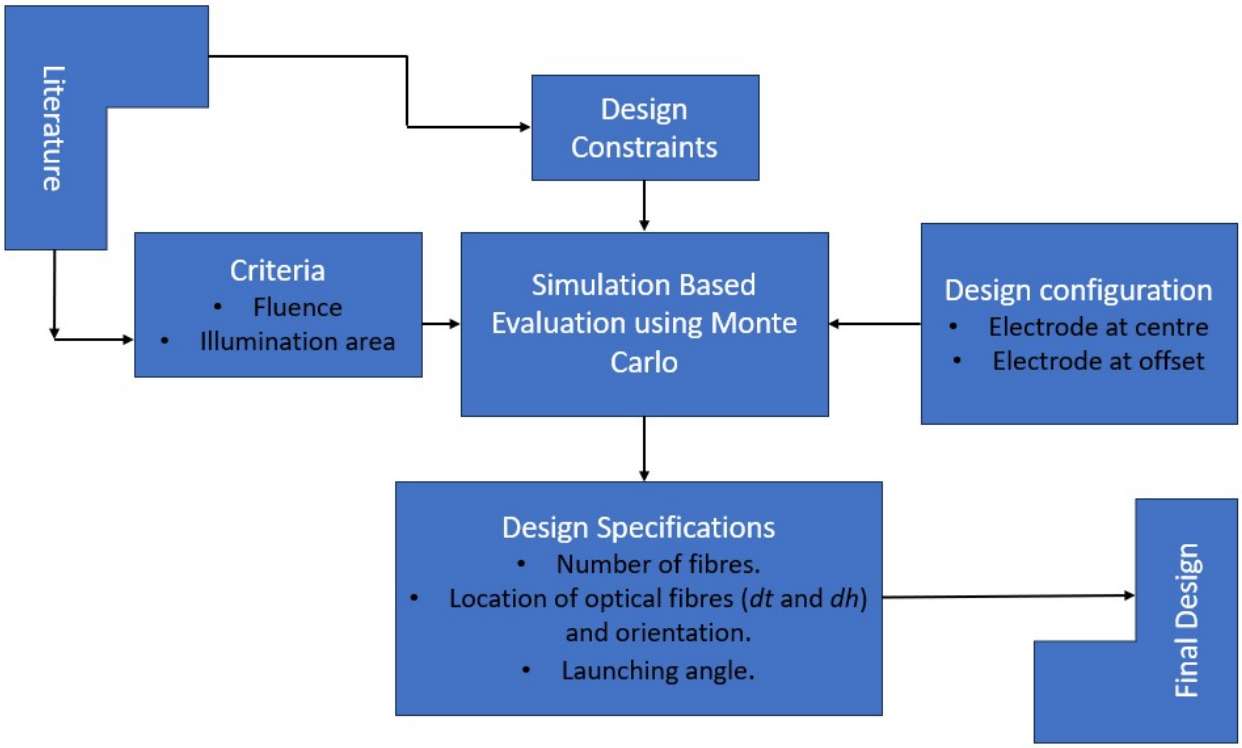

Figure 3.2: Design methodology

3.3 Monte Carlo simulations

Monte Carlo simulations serve as a valuable tool for comprehending variations in fluence levels experienced by the lesion concerning specific factors: (1) the chosen design configuration, (2) the separation distance between the electrode tip and the laser source, and (3) the orientation of the light source and its position relative to the electrode. The simulations were carried out for both sets of design configurations.

The Monte Carlo simulation method systematically traces the path of light emitted from the source within a three-dimensional (3-D) space, voxel by voxel (volumetric Pixel). This process also factors in the optical properties of blood, lesions, and water, along with those of the Electrode. For creating this simulation study a step-by-step process was followed as shown below:-

- Step 1 - Creating tissue profile and device geometry.
- Step 2 - Assigning material and material properties to profile.
- Step 3 - Defining beam.
- Step 4 - Generating results for fluence and illumination area.

These steps are described below in detail.

Geometry formation

The geometry here refers to the catheter geometry that is representative of the design configuration mentioned earlier. The geometric framework was established by constructing layers along the z-axis. The electrode is modeled as a cylindrical layer that can be offset horizontally as required. Likewise, for modeling a lesion, a hemispherical shape was introduced. The layer thicknesses were based on findings from the literature.

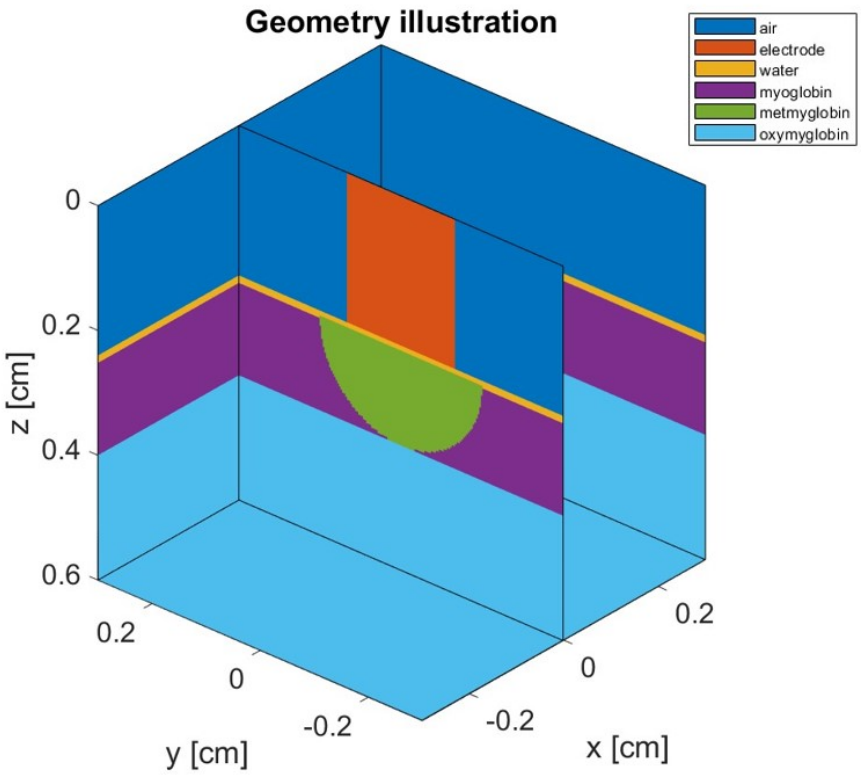

Figure 3.3: Geometry profile of the catheter

Beam definitions

Optical fibers are modeled as point sources adhering to specific beam definitions for simulation purposes. The software offers several options for beam definitions, including:

1. Pencil Beam
2. Isotropically Emitting Line or Point Source
3. Infinite Plane Wave
4. Laguerre-Gaussian (LG01) Beam
5. Gaussian Beam
6. X/Y Factorizable Beam (e.g., Rectangular LED Emitter)

A Gaussian Beam was selected to emulate fiber-like behavior, as laser fibers typically generate a Gaussian distribution. To comprehend Gaussian optics, two key parameters must be examined: angular plane intensity distribution and focal plane intensity distribution. The intensity measure commonly used is the $1/e^2$ of maximum intensity, aligning with American standards for specific applications.

Material properties

The 'mediaProperties' function is responsible for defining all the optical and thermal properties of the media involved. After finalizing the geometry, each component in the profile was assigned its optical properties. To characterize a material, three primary properties are provided: the absorption coefficient, scattering coefficient, and anisotropy.

Absorption Coefficient (μ_a): The absorption coefficient (μ_a) is a measure of how strongly a material absorbs light at a particular wavelength. It quantifies the rate at which light is absorbed as it passes through the material. Mathematically, it represents the fraction of incident light that is absorbed per unit length. Higher values of μ_a indicate greater light absorption by the material. In medical imaging, for instance, μ_a is essential for understanding how various tissues in the body absorb different wavelengths of light. It is also used in techniques like near-infrared spectroscopy and imaging to study tissue properties and oxygenation levels.

Scattering Coefficient (μ_s): The scattering coefficient (μ_s) measures the scattering of light within a material without absorption. It quantifies the rate at which light changes direction due to interactions with small particles or structural irregularities within the material. Higher values of μ_s indicate a greater propensity for scattering. Materials with a high μ_s, like frosted glass, scatter light broadly in many directions. In medical imaging and optics, understanding μ_s is crucial for characterizing how light interacts with tissues or media, particularly in techniques such as diffuse reflectance spectroscopy, which assesses the composition of materials based on how they scatter light.

Anisotropy (g): Anisotropy (g) is a measure of the directional dependence of scattering in a material. It describes whether scattering is predominantly forward (towards the incident direction), backward (opposite the incident direction), or isotropic (scattering occurs uniformly in all directions). Anisotropy is represented by the anisotropy factor, often denoted as g. A value of g close to 1 indicates forward scattering, while a value close to -1 indicates backward scattering. An isotropic material has a value of g near 0. Anisotropy is particularly important in fields like biomedical optics, where it helps describe how light interacts with biological tissues, which can have varying degrees of anisotropy depending on their composition and structure. Understanding anisotropy aids in the accurate modeling of light propagation in tissues for diagnostic and therapeutic purposes.

All the properties are dependent on the wavelength of light. For this study, 790 nm wavelength is chosen [9]. For the electrode platinum is chosen as it is most common in medical devices. The values utilized in the code are obtained from a range of published sources [22] [23] [24] [25]. Given the absence of a theoretical method for obtaining these values, the resulting experimental data tends to exhibit variations. Furthermore, the dependency of these values on numerous other factors contributes to the observed variations. It is important to note that the obtained values may not represent the utmost accuracy in this context.

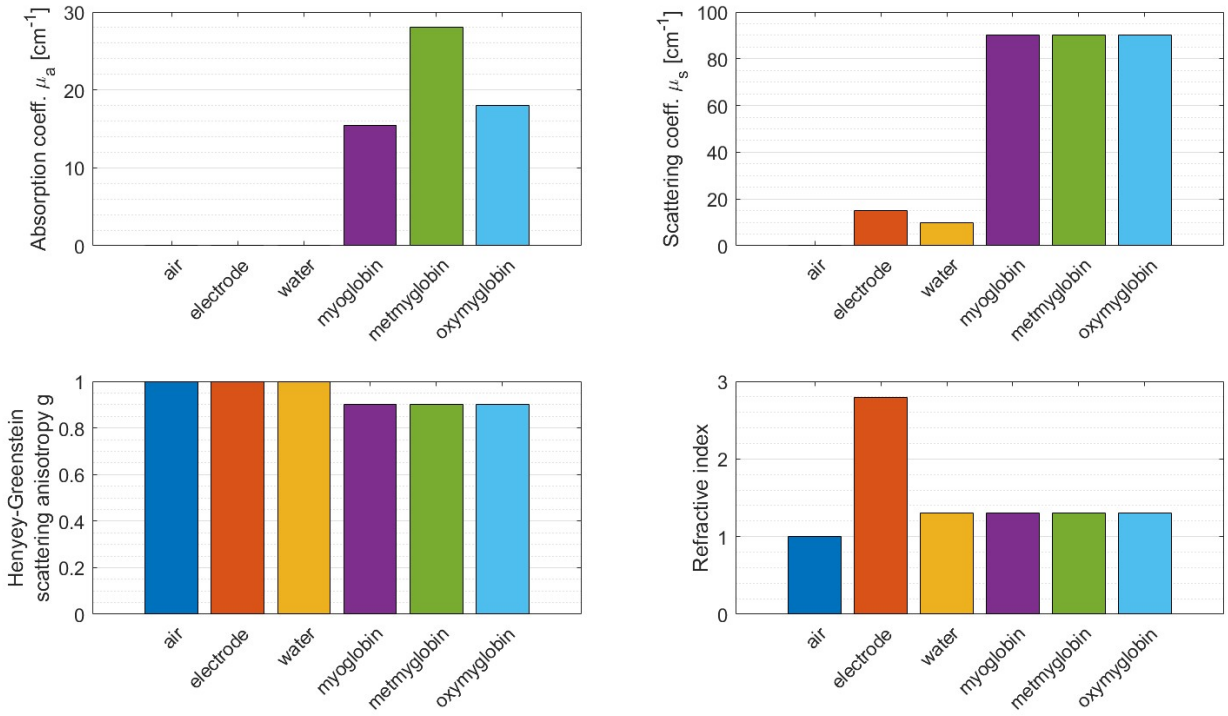

Figure 3.4: Material Properties at 790 nm wavelength

3.4 Results and discussion

Having completed multiple iterations of both design configurations, the final selected values are discussed in this section along with some discussions.

Number of fibers and fiber orientation

The rationale behind the selection of the number of fibers is straightforward. Increasing the number of fibers reduces compliance. Previous results [14] showed that using a single fiber provided insufficient illumination, compromising the continuity of lesion visualization.

Hence, the objective was to orient the fibers in a way that maximized the utilization of the central intensity while covering a broad area with the minimum number of fibers. The initial step in this direction was the utilization of four fibers. The results of employing four fibers in both initial design configurations are presented in Figure 3.6 and Figure 3.7.

For symmetry, the next iteration would require the addition of two more fibers (total 6). This would lead to an excessive amplification of light as well as compromise compliance of the catheter. Furthermore, since the design requirements (in terms of spot size and fluence) were achieved using four fibers, this number was selected. The results of using four and six fibers are shown in the Figure 3.5. It is clearly seen that four fibers are able to achieve the required spot size. The only advantage 6 fibres offer is a uniform and a bigger circular spot.

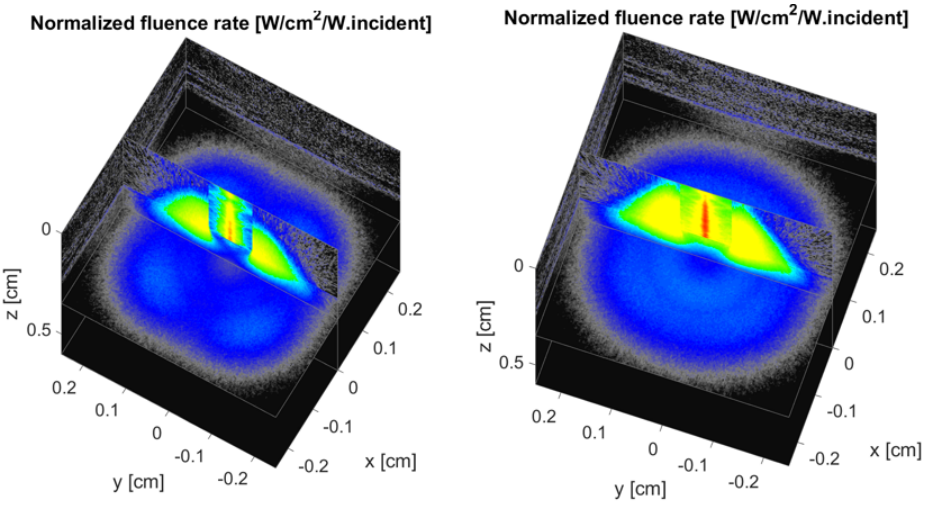

Figure 3.5: Spot size comparison for 4 and 6 fibers respectively

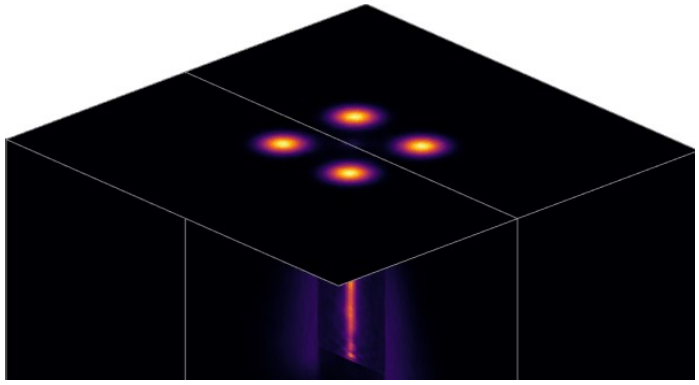

Figure 3.6

For the second design, as the fibers were no longer constrained by the presence of an electrode, there was an opportunity to consider bundling them together. However, it was observed that when bundled, they produced a smaller spot size compared to when they were placed slightly further apart. Consequently, the concept of using bundled fibers was abandoned.

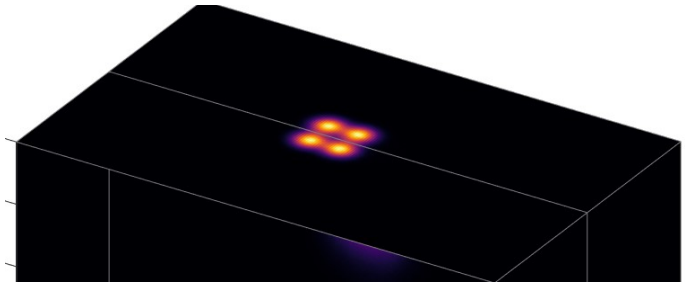

Figure 3.7

Fiber Distance from electrode tip (d_h)

As the distance between the light source and the tissue changes, it is anticipated that the size of the illumination spot will also vary. To investigate this, the position of fibre source was incrementally advanced nearer to the end of the electrode tip. As an initial assumption, the distance between the optical fiber in the XY plane relative to electrode edge 'd_t' was chosen adjacent to the electrode. In the simulation, the illumination area or spot size at a fixed depth of 1 mm from the top of the lesion was monitored. In Figure 3.8 three different values of d_h are shown at $1mm$ increments.

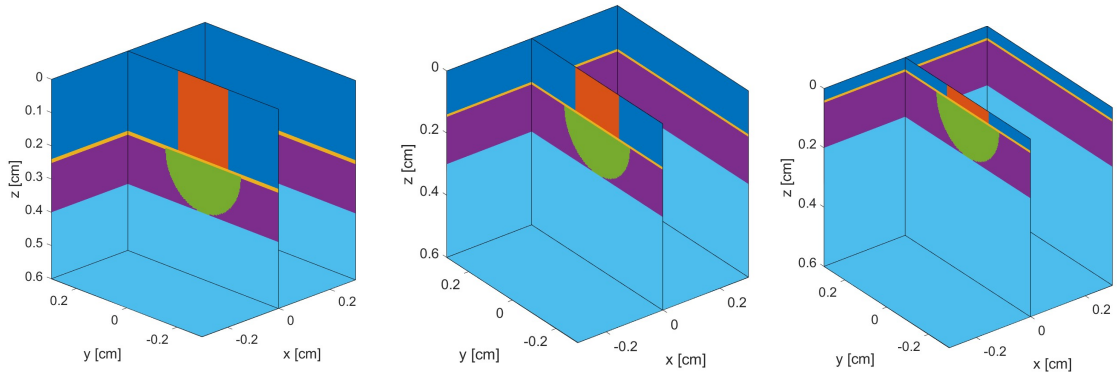

((a)) 2.5 mm ((b)) 1.5 mm ((c)) 0.5 mm

Figure 3.8: Varying the vertical distance of fiber source from electrode tip

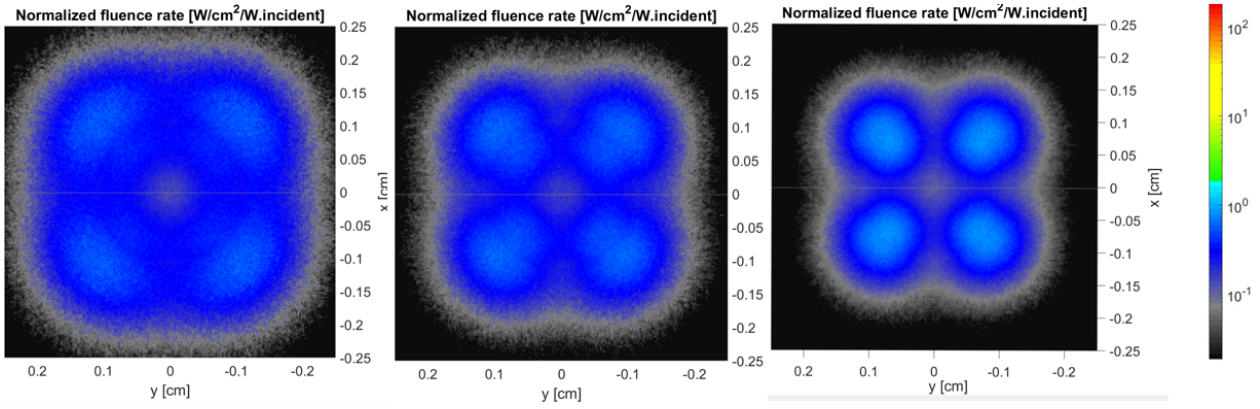

Figure 3.9: Spot size at 1 mm depth of the lesion as the fiber vertical distance from electrode tip increases. (From left to right the distance changes from 2.5 mm to 0.5 mm as seen in geometry)

In the case of the first design, the beam profile is depicted in Figure 3.9. The size of the illumination spot does vary, with the largest spot occurring when the light source is furthest from the electrode tip. While the fluence is most concentrated in the third sub-figure, it does not form a continuous circular spot and has an inconsistent profile.

For the second design, the spot looks different as shown in Figure 3.10. It is able to visualize only half the lesion. The electrode comes in the way and prevents the light from illuminating the black region in subfigure 1.

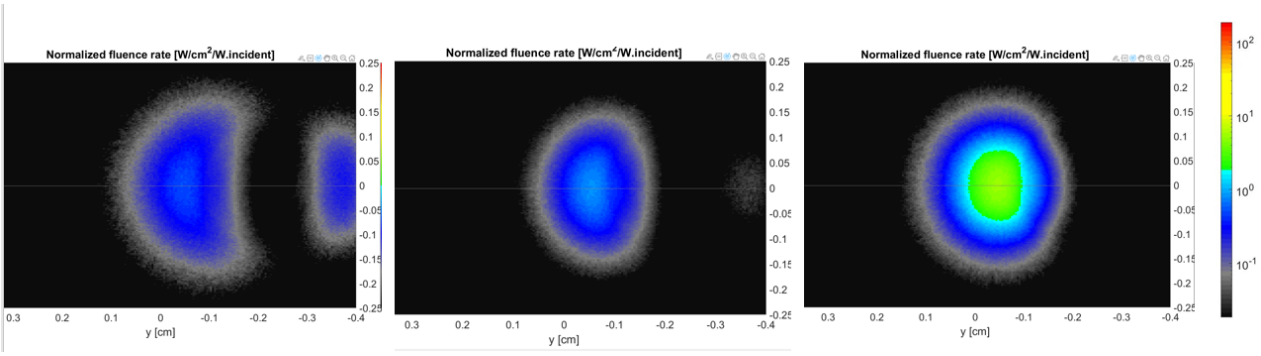

Figure 3.10: Spot size at 1 mm depth of the lesion as the fiber vertical distance from electrode tip increases for design 2 (From left to right the distance changes from 2.5 mm to 0.5 mm as seen in geometry)

Fiber position relative to electrode (d_t)

In the context of the simulation, d_t, the radial distance between the four optical fiber light sources and the electrode, was systematically varied. The objective was to investigate the resulting normalized fluence distribution.

To quantify the fluence distribution, a 3D matrix representation was used. Within this matrix, each voxel corresponds to a discrete volume element, and each voxel holds a fluence value. The analysis focused on a specific region of interest on the x-y plane, which measures 5mm x 5mm and is centered at the electrode. This region was defined to capture the central portion of interest i.e. the lesion and its nearby surroundings. The mean fluence values for the Z-axis at a fixed depth were calculated by considering only those voxels within the 3D matrix that fell within the specified 5mm x 5mm area. These mean fluence values were crucial in characterizing the fluence distribution at that particular depth, taking into account the entire spot size. Figure 3.11 illustrates the outcome of this analysis, giving an idea of the average fluence in this area as the fibers are moved away from the electrode radially.

The graph follows a quadratic function. This indicates that if the position of the source is too close to the fiber, much of the light is blocked by the electrode whereas if it is too far, the lesion area is not properly illuminated. The radius of the electrode is 0.1 cm, this acts as the starting point for the measurement. The peak of the graph is at 0.12 cm which is 200 um from the electrode edge. This implies that for maximal fluence the bare fibre radii must fit within this 200 um threshold. However, there is some leeway possible as the optimized fluence value is considerably higher than the design requirement.

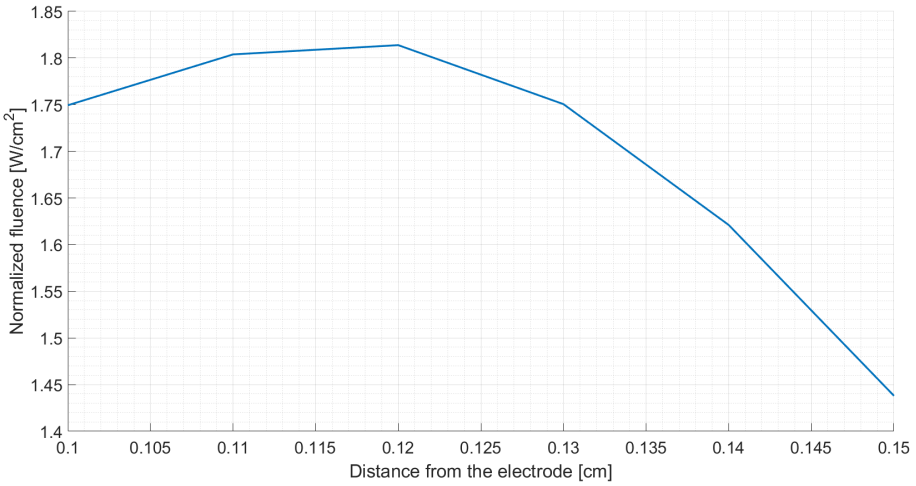

Figure 3.11: Variation of fluence with the distance from the electrode for design 1

For the second design, a similar study was conducted. In this case, the closest distance from the electrode was considered as the initial point and gradually it was moved away from the electrode. The trend in Figure 3.12 indicates that as the source is closing towards the electrode, a drop in its fluence values is absorbed. In fact, the values are way below the values observed in the first design. The variation also depends on the launching angle of the source (that will be covered in the next section) but in general, it does not outperform the first design.

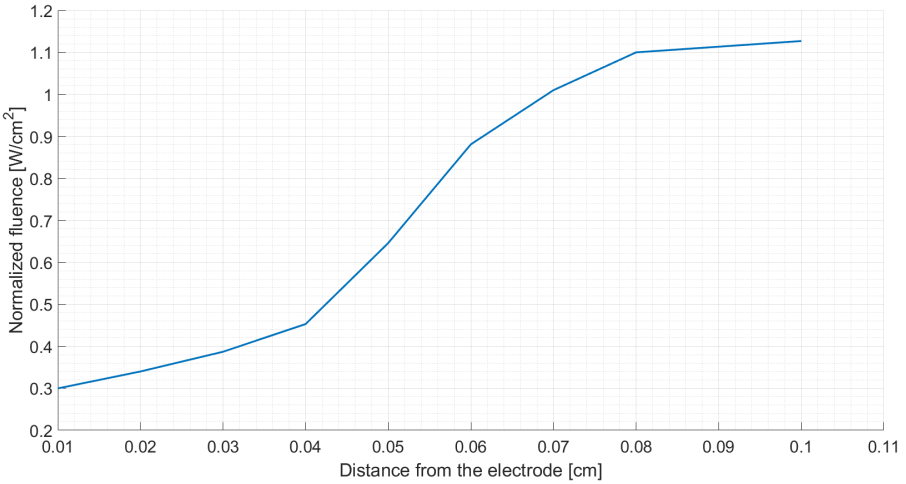

Figure 3.12: Variation of fluence with the distance from the electrode for design 2

Launching angle

The concept of the 'launching angle' is relevant only to the second design, where the electrode is positioned on the side of the catheter. In this configuration, it becomes essential to ensure effective light delivery to the lesion is achieved as shown in the geometry in Figure 3.13.

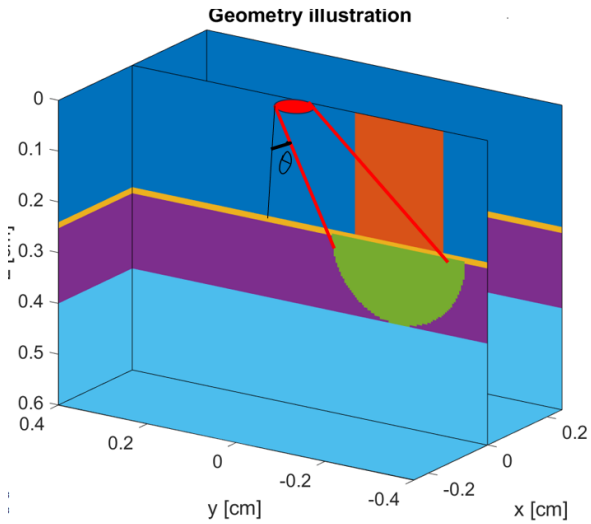

Figure 3.13: Design 2 geometry

To determine the optimal launching angle for this scenario, a light collector element (photodetector) was positioned at the location of the lesion. Simulations were conducted by varying the angle of light delivery. The angle at which the light collector captured the highest fluence was subsequently chosen as the launching angle. The outcomes of these simulations are presented in the following Figure 3.14. It is clearly seen that at pi/8 maximum fluence is achieved and the spot size is bigger too.

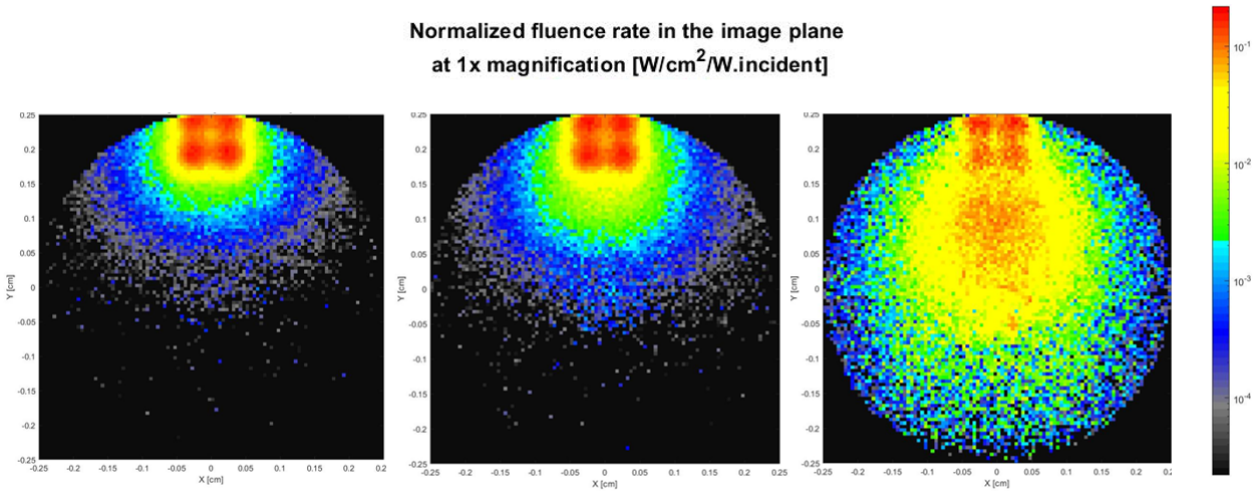

Figure 3.14: Effect of launching angle on fluence for design 2. From left to right the angles in radians are pi/16, pi/10, pi/8

3.5 Final Design

After looking into both design configurations and getting the required values for design parameters, it is observed that

- The number of fibers chosen for both designs is 4.
- For both the designs, varying the distance d_h, It was concluded that the illumination spot size at a fixed depth increases as the distance is increased within a range of 0-2 mm.
- Different results are observed when varying the distance d_t for both designs. For Design 1, the variation follows a quadratic curve, while for Design 2, the further the source from the electrode, the better the fluence achieved.
- The optimal launching angle for design 2 is pi/8 which can be achieved through the use of a micromirror inside the catheter.

The lesion profile for both the designs at their optimal design specifications is seen in Figure 3.15.

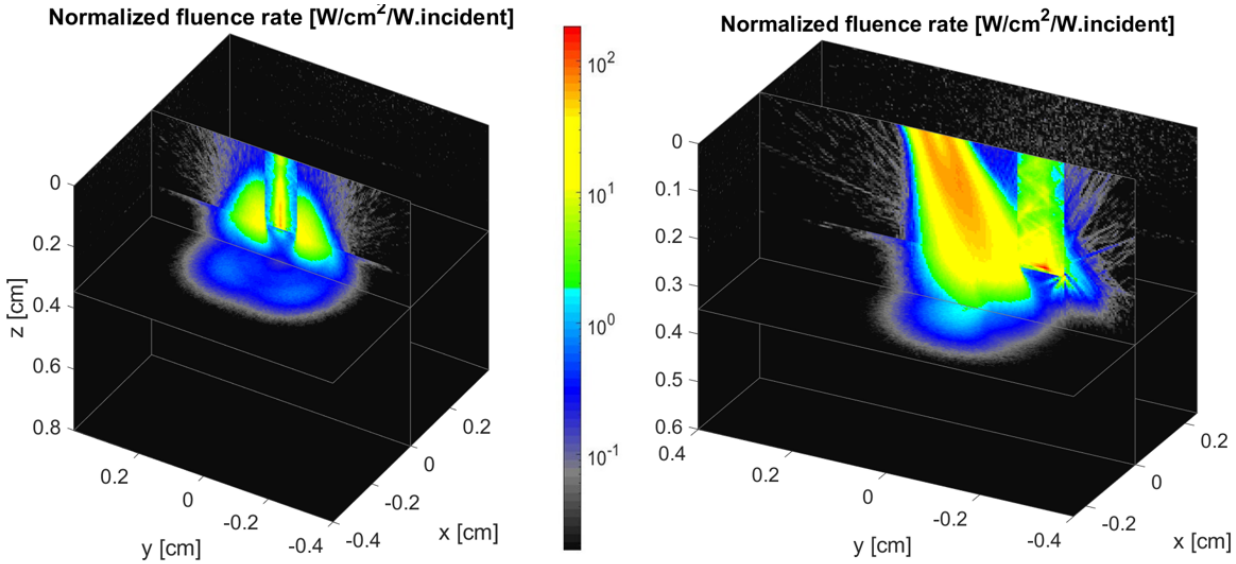

Figure 3.15: Lesion profile for both the designs at their optimal design specifications (from left to right design 1 and design 2 respectively.

It was concluded that the design with an electrode at the center generally performs better in all aspects when compared to the one with the electrode at an offset. The optimum distance from the catheter tip to source d_h is $2mm$, while the optimum position of fiber relative to catheter d_t is $200um$. The number of fibres used is 4 and the launching angle for this configuration remains perpendicular to the catheter. A CAD model having these design specifications was created and is illustrated in Figure 3.16 and Figure 3.17. The model also showcases a possible packaging configuration for all the components combined including the electrode, the optical fibers, the force sensor, the ultrasound transducers, the catheter casing, and all the supplementary wiring of each component which will extend till the proximal end of the catheter.

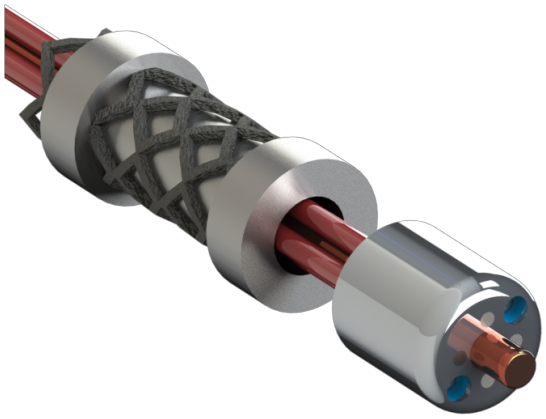

Figure 3.16: CAD model of the catheter with covering and force sensor hidden

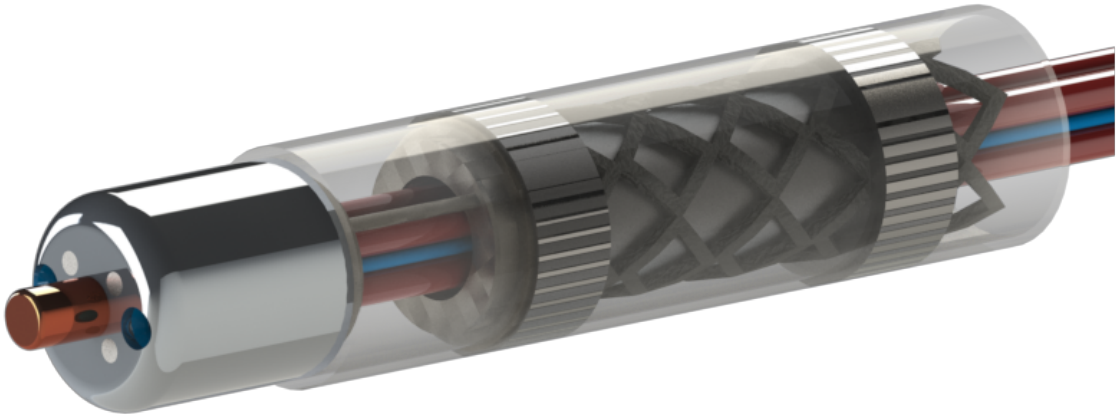

Figure 3.17: CAD model of complete catheter assembly proposal

4 | Experiment Methods

The experimental phase of this thesis focuses on the development of tools to validate beam profile from optical fibers and its comparison with simulation results. The primary objective of the experiment is to validate the orientation and the design specification of the first design configuration which was selected from the previous chapter, ensuring their capability to generate the expected profile observed in the simulation. By confirming that the desired beam profile is achieved at the catheter's output, we establish that the light delivery system closely adheres to the simulated path, accounting for material properties. This initial phase validation serves as a valuable step in affirming the usability of the current catheter design. In this section the experimental setup will be discussed that highlights the development of tools to carry forward this experiment in the future.

4.1 Experimental setup

For the experimental setup, a free-space laser generator was employed, producing a coherent laser source with an almost elliptical beam shape. Two deflectable mirrors were used to precisely steer the laser path, and attenuators were included in front of the laser source to protect the fibers from potential damage.

To couple the free-space laser into the fiber, a single multimode fiber was initially used. Since the beam diameter greatly exceeded the core diameter of the fiber, a converging lens was used to reduce the beam diameter, aligning it as closely as possible with the fiber's numerical aperture. A lens with a focal length of 250 mm and a fiber connector near its focal point was employed for this purpose. The presence of a fiber jacket and connector allowed for easy connection and power monitoring.

Subsequently, an Edmond optics beam profiler was utilized to obtain comprehensive measurements of the beam profile, spot size, and intensity.

This constituted the basic setup. However, when it came to testing the catheter designs, a significant challenge arose in achieving the required fiber orientation. The use of conventional fibers with jackets and connectors did not provide the necessary flexibility for alignment. Since experimental validation needed to closely resemble the actual catheter design, a method was required to replicate the same geometry and structure. Additionally, efficiently coupling multiple fiber sources with an efficiency exceeding 60 percent posed another challenge.

To address these issues, bare laser fibers were employed due to their compact size and orientation flexibility.

An SLA 3D-printed microstructure was designed to securely hold the bare fibers while providing the required angles.

Figure 4.1: 3d printed part mimicking the catheter tip design

The step-by-step procedure is as follows:-

- Step 1 - Align the free space laser.

  Aligning the laser beam is the first step. It is to maximize power transfer, minimize losses, preserve beam quality, ensure safety, and obtain reliable and accurate results in various applications. To check if the laser is aligned, a power meter is used. By measuring power across different points in the optical path a change in the power is observed that can give an indication about alignment.

- Step 2 - Clean and cleave the fiber.

  Bare fibers need to be cleaved to be able to be used for coupling to facilitate the propagation of light without contamination. To cleave fibers, a separate device is used which cuts perfectly through the fiber in a manner that the glass undergoes a clean cut. The end parts of the fiber that need to be cleaved should be stripped off from their cladding before cleaving as seen in Figure 4.2.

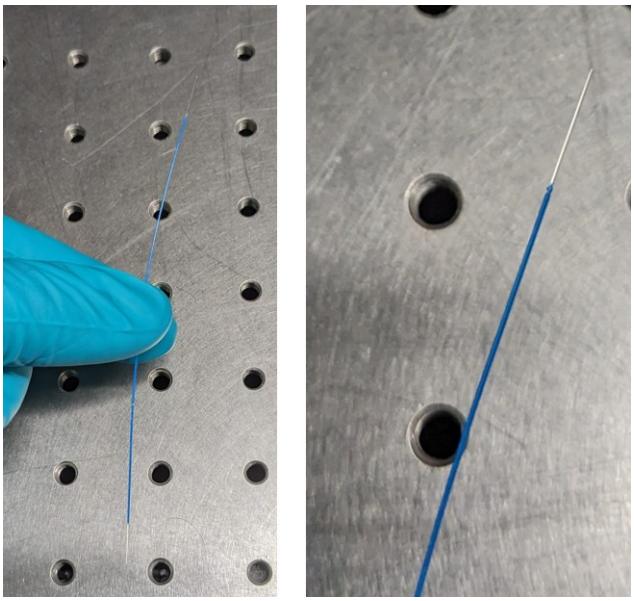

Figure 4.2: fiber stripped to its core from cladding at both ends

- Step 3 - Couple the fiber.

  The most important step is to couple the laser beam with the laser fiber. As discussed, for this step 3d printed parts were designed that have the same orientation as the design. In order to get micrometer precision, SLA printer technology was used. A converging lens was used to reduce the beam diameter as we want most of the light to be inside the fibers, the beam diameter must be reduced to around $3.5mm$ so that proper efficiency can be achieved and all four fibers get coupled. Two structures were printed, one for the laser side where light first enters the fiber and the other at the distal end that mimics the design of the catheter. In order to improve the result, a pinhole with two lenses was set. This reduced the beam diameter and gave much more precision over the results.

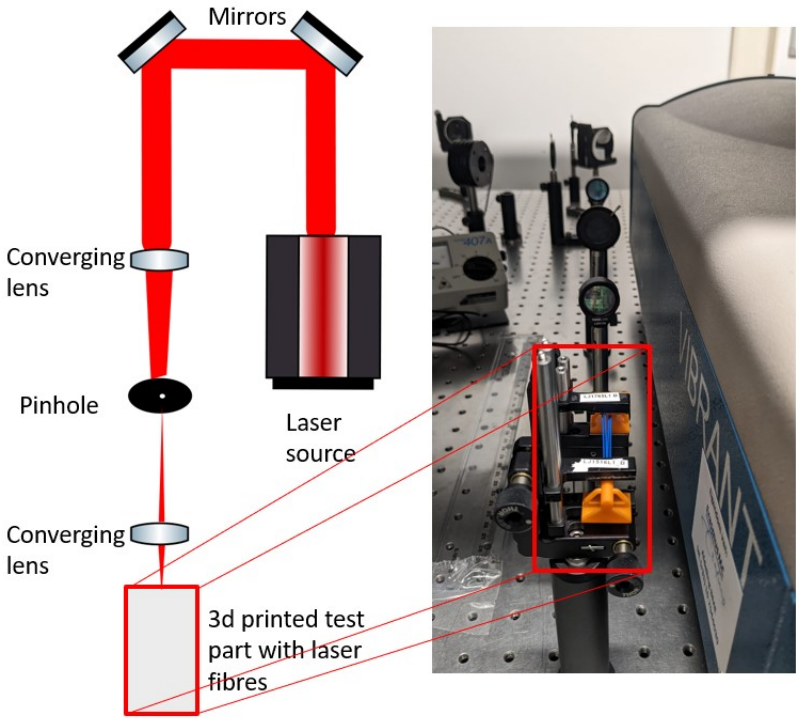

Figure 4.3: Experiment Setup

- Step 4 - Connect the beam profiler and observe the results After aligning and coupling the fibers, a beam profiler is used to observe the distribution of laser power across the beam's cross-section.

5 | Conclusions and Recommendations

5.1 Conclusions

The primary objective of this research was to address the design of integrated photoacoustic catheters, particularly the light delivery system in such a way that it gives enough fluence at a fixed depth to illuminate an area of at least $4.5mm$ to monitor lesions effectively. A simulation-based approach using Monte Carlo simulation was proposed. This approach proves to be suitable for photoacoustic light delivery as the light is represented as photon packets that gradually get absorbed as they traverse the medium, which is how the photoacoustic phenomenon works.

The Monte Carlo simulation was successfully implemented to inform the design specifications for the light delivery of an integrated photoacoustic catheter. The design presented in this thesis is optimized for the Radiofrequency electrode positioned at the center of the catheter. For a 7F ($2.33mm$) diameter electrode, the optimal fiber vertical distance from the electrode tip to the fiber source was identified as $2mm$. At this optimal distance, four symmetric fibers were each positioned at a radial distance of $200um$ from the edge of the electrode with a launch angle of 90 degrees. This design configuration meets all the sought-after specifications.

The variation of fluence and spot size over different fibre source positions were also found which can be used to determine any future changes in the design. These relations also give an idea of which fiber is suitable to use in order to fabricate a product. The advantage of using a simulation-based approach is it can applied to a multitude of custom design configurations/-concepts. It is a good tool to have before the experimentation stages as it gives an estimation of design values and saves the effort and time that multiple experimental iterations take.

Finally, SLA 3D printed parts were successfully developed to mimic the design, serving as prototypes for testing the simulation results. The resolution offered by SLA 3D printing technology proved suitable for generating holes for bare fibers and facilitating the coupling of the free space laser with the 3D printed components.

Although, this approach is good for a preliminary idea of the design specifications, it fails to account for the reality of components. For example, according to the simulation, the best design will be the one where the electrode is 1 mm in diameter, which is possible but it is not ideal in this specific case. Likewise, the simulation will not yield the exact requirements for a product such as which fibre to use, what should be the numerical aperture of that fibre. It will simply be able to give a light source profile and it is up to the researcher to determine how this source could be generated. Secondly, it does not give any information regarding the

acoustic waves that are received back which is only possible through experimentation. Lastly the material properties used in this study are experimental results, the assumption that the experiment will follow the simulation path is not a guarantee.

This research presents a valuable contribution to the field of photoacoustic imaging by introducing a simulation-based approach to address challenges related to the design of catheters. This approach opens up exciting opportunities for further exploration and application, promising to expand the capabilities and reliability of catheter ablation procedures.

5.2 Recommendations

The proposed method offers significant advantages; however, like any research, there is always room for further improvements and extensions. These recommendations are as follows:

- Generate a beam profile with the proposed experiment setup and calculate the coupling efficiency of the 3d printed part.
- The initial experiments done in this research prove the use of SLA 3D printing technology to test light delivery, but it doesn't account for the interference of electrodes that come in the way of the light delivery as seen in simulations. Furthermore, the experimental validation could be done with the whole photoacoustic setup involving a phantom for tissue and ultrasound transducers, which will give an idea about the Signal-to-noise ratio and contrast-to-noise ratio of the generated images.
- The Monte Carlo simulation can also be used to simulate heat profiles just like fluence profiles. This will give the physicians valuable information about temperature profiles at depth. Along with heat profiles, a model for when the catheter is at different catheter-tissue angular positions.
- The simulation study can be turned into an engineering optimization problem to maximize fluence with design variables being the positioning of the electrode and fibers and constraints being the physical design constraints.

Bibliography

[1] "What happens when the heart is in atrial fibrillation?" *StopAfib.org*. [Online]. Available: https://www.stopafib.org/learn-about-afib/what-is-afib/about-the-heart/

[2] "Cardiac ablation procedure for arrhythmia," *UChicago Medicine*. [Online]. Available: https://www.uchicagomedicine.org/conditions-services/heart-vascular/arrhythmias/ablation-therapy

[3] J. A. E. Spaan, J. M. T. de Bakker, and M. J. Janse, *Feedback Mechanisms in Ablation Catheters*. Springer, 2007.

[4] E. Marijon, S. Fazaa, K. Narayanan, B. Guy-Moyat, A. Bouzeman, R. Providencia, F. Treguer, N. Combes, A. Bortone, S. Boveda, S. Combes, and J.-P. Albenque, "Real-Time Contact Force Sensing for Pulmonary Vein Isolation in the Setting of Paroxysmal Atrial Fibrillation: Procedural and 1-Year Results," *J Cardiovasc Electrophysiol*, vol. 25, pp. 130–137, 2014. [Online]. Available: https://onlinelibrary.wiley.com/doi/10.1111/jce.12303

[5] J. S. Chinitz, G. F. Michaud, and K. Stephenson, "CATHETER ABLATION Impedance-guided Radiofrequency Ablation: Using Impedance to Improve Ablation Outcomes."

[6] T. Lin, F. Ouyang, K.-H. Kuck, and R. Tilz, "ThermoCool® SmartTouch® Catheter – The Evidence So Far for Contact Force Technology and the Role of VisiTag™ Module," *Arrhythmia & Electrophysiology Review*, vol. 3, no. 1, pp. 44–47, 4 2014.

[7] V. Tiporlini, S. Ahderom, P. Pratten, and K. Alameh, "Advanced fully integrated radiofrequency/optical-coherence-tomography irrigated catheter for atrial fibrillation ablation," 2020. [Online]. Available: https://doi.org/10.1002/jbio.202000243

[8] K. Masnok and N. Watanabe, "Catheter contact area strongly correlates with lesion area in radiofrequency cardiac ablation: An ex vivo porcine heart study," *Journal of Interventional Cardiac Electrophysiology*, vol. 63, 04 2022.

[9] S. Iskander-Rizk, P. Kruizinga, A. F. W. van der Steen, and G. van Soest, "Spectroscopic photoacoustic imaging of radiofrequency ablation in the left atrium," *Biomedical Optics Express*, vol. 9, no. 3, p. 1309, 2018.

[10] X. Yang, Y. H. Chen, F. Xia, and M. Sawan, "Photoacoustic imaging for monitoring of stroke diseases: A review," *Photoacoustics*, vol. 23, p. 100287, 9 2021.

[11] R. Bouchard, N. Dana, L. Di Biase, A. Natale, and S. Emelianov, "Photoacoustic characterization of radiofrequency ablation lesions," *Photons Plus Ultrasound: Imaging and Sensing 2012*, vol. 8223, no. February 2012, p. 82233K, 2012.

[12] N. Dana, L. Di Biase, A. Natale, S. Emelianov, and R. Bouchard, "In vitro photoacoustic visualization of myocardial ablation lesions," *Heart Rhythm*, vol. 11, no. 1, pp. 150–157, 2014. [Online]. Available: http://dx.doi.org/10.1016/j.hrthm.2013.09.071

[13] "Cardiovasc electrophysiol - 2014 - PANG - Three-Dimensional Optoacoustic Monitoring of Lesion Formation in Real Time During.pdf."

[14] S. Gao, A. Rahaman, H. Ashikaga, H. R. Halperin, and H. K. Zhang, "Miniaturized Catheter-Integrated Photoacoustic Ablation Monitoring System: A Feasibility Study," *IEEE International Ultrasonics Symposium, IUS*, vol. 2022-Octob, pp. 2–5, 2022.

[15] S. Gao, H. Ashikaga, M. Suzuki, T. Mansi, Y.-H. Kim, F.-C. Ghesu, J. Kang, E. M. Boctor, H. R. Halperin, and H. K. Zhang, "Cardiac-Gated Spectroscopic Photoacoustic Imaging for Ablation-Induced Necrotic Lesion Visualization: In Vivo Demonstration in a Beating Heart," *bioRxiv*, p. 2022.05.23.492682, 2022. [Online]. Available: https://www.biorxiv.org/content/10.1101/2022.05.23.492682v1%0Ahttps://www.biorxiv.org/content/10.1101/2022.05.23.492682v1.abstract

[16] M. Basij, S. John, D. Bustamante, L. Kabbani, W. Maskoun, and M. Mehrmohammadi, "Integrated Ultrasound and Photoacoustic-Guided Laser Ablation Theranostic Endoscopic System," *IEEE Transactions on Biomedical Engineering*, vol. 70, no. 1, pp. 67–75, 2023.

[17] S. Iskander-Rizk, G. Springeling, P. Kruizinga, R. H. Beurskens, A. F. Van Der Steen, and G. Van Soest, "Photoacoustic-Enabled RF Ablation Catheters for Lesion Monitoring," *IEEE International Ultrasonics Symposium, IUS*, vol. 2018-Octob, 12 2018.

[18] S. Iskander-Rizk, P. Kruizinga, R. Beurskens, G. Springeling, F. Mastik, N. M. de Groot, P. Knops, A. F. van der Steen, and G. van Soest, "Real-time photoacoustic assessment of radiofrequency ablation lesion formation in the left atrium," *Photoacoustics*, vol. 16, no. October, p. 100150, 2019. [Online]. Available: https://doi.org/10.1016/j.pacs.2019.100150

[19] J. Rebling, F. J. Oyaga Landa, X. L. Deán-Ben, A. Douplik, and D. Razansky, "Integrated catheter for simultaneous radio frequency ablation and optoacoustic monitoring of lesion progression," *Optics Letters*, vol. 43, no. 8, p. 1886, 2018.

[20] M. Basij, S. John, D. Bustamante, L. Kabbani, and M. Mehrmohammadi, "Development of an Integrated Photoacoustic-Guided Laser Ablation Intracardiac Theranostic System," *IEEE International Ultrasonics Symposium, IUS*, pp. 2021–2024, 2021.

[21] P. E. Andersen, A. K. Hansen, D. Marti, R. N. Aasbjerg, P. E. Andersen, A. K. Hansen, M.-i. Monte, D. Marti, R. N. Aasbjerg, P. E. Andersen, and A. K. Hansen, "dimensional Monte Carlo light transport solver with heat diffusion and tissue damage heat diffusion and tissue damage," vol. 23, no. 12, 2023.

[22] W. J. Bowen, "The absorption spectra and extinction coefficients of myoglobin." *The Journal of biological chemistry*, vol. 179 1, pp. 235–45, 1949. [Online]. Available: https://api.semanticscholar.org/CorpusID:2528224

[23] T. Nguyen, Jae, and G. Kim, "A simple but quantitative method for non-destructive monitoring of myoglobin redox forms inside the meat," *Journal of Food Science and Technology*, vol. 56, 2019. [Online]. Available: https://doi.org/10.1007/s13197-019-04006-y

[24] R. P. Institute, "Refractive index and extinction coefficient of materials," pp. 1–276, 2004. [Online]. Available: https://sites.ecse.rpi.edu/~schubert/Educational-resources/Materials-Refractive-index-and-extinction-coefficient.pdf

[25] L. Lin, J. Yao, L. Li, and L. Wang, "In vivo photoacoustic tomography of myoglobin oxygen saturation," *Journal of biomedical optics*, vol. 21, p. 61002, 12 2015.